

Effect of side frictions in a centrifuge model of slope sliding along a bedding plane

○Krit AROONWATTANASKUL, Thirapong PIPATPONGSA, Takafumi KITAOKA, Hiroyasu OHTSU

To understand more about the effect of side frictions, this study examines an empirical estimation of the side frictions effect on a slope sliding along a bedding plane by using a failure envelope. Two series of experiments; slope width 20 cm and 40 cm, were conducted with a variation of thickness, slope length, and slope angle. The results of the slope width 40 cm were employed to predict centrifugal acceleration at the failure of the slope width 20 cm model. The relationship between normal force and driving force was obtained experimentally to validate the former predictive value.

1. Introduction

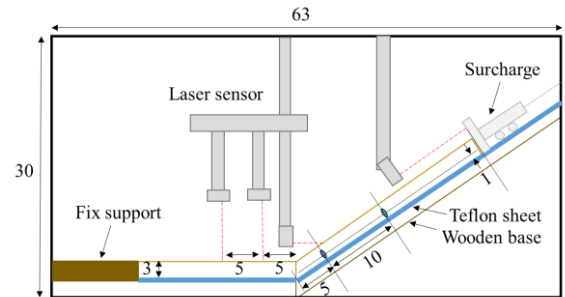
In the process of studying the behavior of soil structures using centrifuge modeling, the model boundaries provide side frictional supports the model, and this effect may lead to an uncertain prediction when extrapolated to a prototype scale. The lubrication systems in laboratory tests, i.e., grease method and plastic sheet method (Fang et al., 2003) have been studied to improve aforementioned problem. However, these systems could not eliminate lateral friction due to difficulty in controlling the experimental procedures; a better understanding of the effect of side frictions is still necessary.

2. Methodology

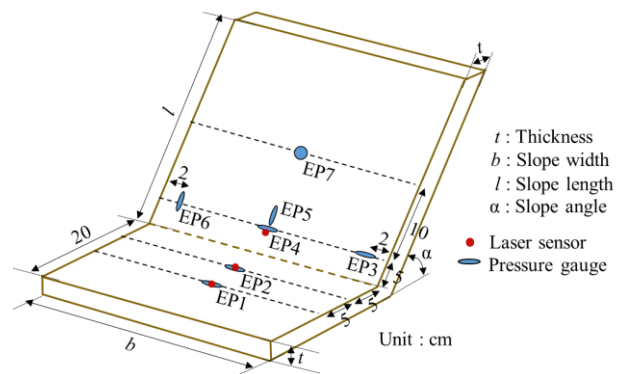
Table 1 Basic properties of Edosaki sand and interface

Bulk unit weight ( $\gamma$ )	18.2 kN/m <sup>3</sup>
Unconfined compressive strength ( $\sigma_c$ )	5.8 kN/m <sup>2</sup>
Interface friction angle ( $\phi_i$ )	14.7°
Apparent adhesion ( $c_i$ )	0.2 kN/m <sup>2</sup>
Internal friction angle ( $\phi$ )	44.2°

The physical models were made of moist Edosaki sand. The basic properties of Edosaki sand and its interface with Teflon sheet are shown in Table 1. The model configuration and structure of the instrument is shown schematically in Fig. 1(a). The model was divided into two parts, basal support, and slope part. Basal support and slope part were placed on a rigid plane covered by a Teflon sheet for simulating the low friction interface plane. Moist sand with an optimum water content of  $w = 15.1\%$  was compacted to achieve a bulk density of  $\rho = 1860 \text{ kg/m}^3$ . Pressure gauges were installed in the slope part during the compaction. Testing conditions were varied by thickness, slope width, slope length and slope angle.



(a) Model configuration



(b) Instrumented slope model

Fig. 1 Slope model with instrumentations

After the preparation of basal support and slope part, a uniform displacement boundary using surcharge was

applied at the slope top edge by using the fabricated wooden roller with a deadweight container. Four laser sensors were installed in various positions (Fig.1(b)) for different objectives, e.g., investigating the upheaval at basal support and monitoring slope displacement. During the test, the centrifugal acceleration was gradually increased until 50g at each surcharge load while monitoring the initial collapse of the model. The centrifugal acceleration was increased until the first failure occurrence.

### 3. Results and discussions

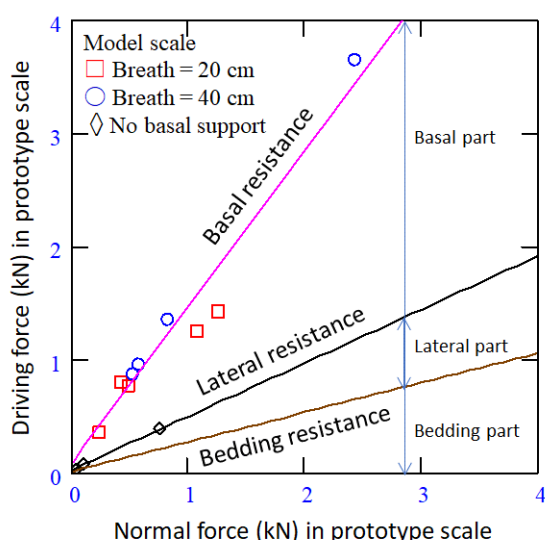


Fig. 2 Experimental result with linear regression

The equilibrium of a slope was simply evaluated by the equilibrium of force along the bedding plane. The forces applying to the slope are the normal and the driving forces. The failure envelope can be determined and plotted in terms of the normal and driving forces per unit contact area of a model along a bedding plane in prototype scale as shown in Fig. 2. Using data obtained from slope width 40 cm experiments (circle symbol) to approach the linear regression (blue line) for predicting the test results in slope width 20 cm. The derived expression shows an acceptable agreement with the experiments. Some data which lie out of the range represents testing results which either failed by different failure mode or retest many times.

The gaps between each line represent the effect of resistance on each part. An example of the predicted and experimental value in the slope width 20 cm model is listed in Table 2. The prediction of an unknown value calculated by using a constant value of other parameters in the following equations.

$$F_N = \rho \times l \times b \times t \times \cos(\alpha) \times n \times g$$

$$F_D = [\rho \times l \times b \times t \times \sin(\alpha) + \Delta m \times (\sin(\alpha) - \tan(\phi_r) \times \cos(\alpha))] \times n \times g$$

$$F_D = c_1 \times F_N + c_2$$

where  $F_N$ : Normal force per unit area,  $F_D$ : Driving force per unit area,  $\Delta m$ : surcharge,  $\phi_r$ : roller's friction angle,  $n$ : centrifugal acceleration,  $g$ : gravitational acceleration,  $c_1$ : gradient and  $c_2$ : y axis-intercept.

Table 2 Predicted and experimental value

Parameters	Predicted value	Experimental value
Centrifugal acceleration ( $n$ )	23.3	28.4

The failure mode in a long slope length model (30cm) occurred Pop-up wedge failure (Fig.3(a)) while those in a short slope length model (20cm) occurred Fore-thrust failure only (Fi.g.3(b)). Experimental results confirm that different failure modes would occur caused by variation of slope length. Therefore, the length of the slope needs to be considered in the design purpose because it also affects slope stability.



a) Slope length 30 cm      b) Slope length 20 cm

Fig. 3 Modes of failure

### Reference

Fang, Yung-Show, et al. "Reduction of boundary friction in model tests." *Geotechnical Testing Journal* 27.1 (2004): 3-12

